Princeton University
Department of Physics

Senior Thesis
Draft of Content

Effects of dark matter self-interaction on the evolution of the Sagittarius stream

Connor Hainje

Advised by
Prof. Mariangela Lisanti

This paper represents my own work in accordance with University regulations.
/s/ Connor Hainje

Abstract

We present a novel study of the Sagittarius (Sgr) tidal stream, investigating the impacts of self-interacting dark matter (SIDM) models to determine their effects on the evolution of this stream. This is done by performing high resolution simulations of the infall of the Sgr galaxy using CDM and SIDM models. The resulting streams are analyzed and compared. Comparisons are also made with observed Sgr candidates from the Gaia DR2 survey.

Contents

Chapter 1

Introduction

1.1 Dark matter

One of the most important unsolved problems in physics is the missing mass problem [1]. It was first identified by Oort while studying galactic rotation curves, where he found that the rotation curve increased linearly with radius, an indication of a constant mass density, despite the fact that the amount of visible matter fell off. The same trend was found in many other galaxies over the following years, indicating that the missing mass problem was not specific to the galaxy Oort was studying.

The peculiar rotation curves led researchers to explore a few possible solutions [2]. The first: perhaps our theory of gravity fails on galactic scales and needs modification. This approach would turn out to fail in large part because it requires modifying general relativity in a manner that remains consistent at *all* scales. The second: perhaps there is some other force at work that modifies the galactic dynamics to produce this phenomenon. This again would be discarded, as there is no other evidence for such a force to exist. The third, and widely considered to be "true", solution is that there is some form of unseen matter about the galaxies that keeps the mass density constant with increasing radius. Because this matter does not interact with the standard model in a way that allows it to be seen, it is known as "dark matter" (DM).

As time has continued, evidence for dark matter has been found in a number of different astrophysical and cosmological data. One such phenomenon is gravitational lensing, whereby a large distribution of matter can bend the path of light in a measurable way. Observed gravitational lensing caused by galaxies and galaxy clusters is in general stronger than would be expected from visible matter alone, but is consistent with the existence of dark matter in the same quantities as predicted by the rotation curves [3]. These and other cosmological data have converged on a "standard model of cosmology" which includes the

existence of dark matter as an important component of the universe.

1.2 Standard cosmological model

The standard cosmological model is the ΛCDM model. This model treats the universe as consisting primarily of three components: the cosmological constant Λ describing the energy density of vacuum, cold dark matter (CDM), and ordinary matter. Of chief relevance for our study is the CDM component, which this model takes to be "cold"—moving at speeds much slower than the speed of light—and collisionless—interacting with itself and other particles through gravity alone.

The ΛCDM model is known as the standard cosmological model because it is a simple model able to account for many of the dominating cosmological phenomena. In particular, its predictions of the existence of the cosmic microwave background agree with observation, it easily accounts for the accelerating expansion of the universe, and it can explain the hierarchical large-scale ($\gtrsim \mathcal{O}(\text{Mpc})$) structures of the distribution of galaxies, like galaxy clusters, superclusters, etc. Despite these strengths, however, one of its largest discrepancies with observation occurs in the small-scale structures of galaxies.

There are several *small-scale problems* that have been discovered in high resolution simulations of the ΛCDM paradigm. Some of the most prominent ones are discussed below, following the discussion of [4].

- The *core-cusp problem*: in simulation, CDM halos generally evolve to have a "cuspy" mass density profile—one which goes like $1/r$ (for r the radius) near the galactic center. The observed rotation curves of many galaxies, however, indicate "cored" mass density profiles—ones which are constant with radius near the center.
- The *missing satellites problem*: CDM halos evolve from the mergers of small halos and thus should have a rich substructure. As such, simulations can be used to obtain predictions about the substructure and, in particular, the number of subhalos (satellite galaxies) that should be present in and about galaxies of certain sizes. However, observations of the Milky Way show that there are far fewer satellite galaxies than are predicted by simulation.
- The *diversity problem*: CDM models predict a remarkably self-similar process for structure formation, indicating that halos of a similar mass should have similar structure. Observations, however, show that many disk galaxies with similar halo mass have relatively large discrepancies in their interior structure and core densities.
- The *too-big-to-fail problem*: The brightest satellite galaxies in the Milky Way are expected to host the most massive subhalos. However, CDM simulations predict the most massive subhalos for a galaxy the size of the

Milky Way to be far too dense to be consistent with the stellar dynamics of observable satellite galaxies. However, subhalos of the predicted mass and density are "too big to fail" in forming observable galaxies, leaving us to wonder what happened to these massive subhalos.

There are a few possible alternatives to the ΛCDM model that are being investigated. These alternatives generally involve considering different forms of dark matter to account for these discrepancies in the small-scale structure. Some researchers believe that the culprit is that most major CDM simulations are DM-only, meaning that the small-scale structure would be validated by the inclusion of baryonic processes. However, many believe that baryonic processes are not significant enough to solve this problem. Another possibility is the consideration of "warm" DM, which yields interesting predictions for the influences of dark matter at earlier times in the universe. A third possiblity, and the one with which we primarily concern ourselves for this study, is that the DM may have a mechanism for self-interaction. This possibility will be covered in more detail in Chapter 2.

1.3 Sagittarius stream

In this paper, we largely consider the Sagittarius (Sgr) satellite galaxy of the Milky Way. Sgr is a dwarf spheroidal (dSph) galaxy orbiting the MW. It is a "dwarf" galaxy due to its low absolute magnitude, a measure of its brightness, and it is "spheroidal" due to its luminosity (opposed to "elliptical") [5]. It was first discovered by Ibata et al. in 1994 [6].

Since its discovery, Sgr has been the subject of many studies due to a few interesting features of its past. It is one of the nearest dwarf galaxies in the MW, making it somewhat easier to obtain detailed measurements for [7]. It is also widely believed to have made several passages through the MW disk over its orbits [8]. This fact in particular makes it greatly interesting, as these orbits have resulting in the stripping of stars from Sgr by the tidal forces of MW gravity, leaving a stream of Sgr debris which wraps the MW completely [8, 9].

The evolution of the Sgr stream is evidently quite sensitive to changes in the MW gravitational potential, the Sgr progenitor mass, and other properties of the galaxies. As such, its study could prove very insightful for obtaining a better understanding of these properties. It is difficult, however, to reconstruct the Sgr orbital history, because different histories are possible when one varies the Sgr mass [10]. The most prominent models have been those due to Law & Majewski [9] and Purcell et al. [8]. More recently, however, a high resolution simulation study was performed that used "live", i.e. dynamic, gravitational potentials for *both* MW and Sgr [11]. This study is the one on which we base the majority of our simulation work.

One unexplored parameter that would necessarily impact the evolution of the Sgr stream is the DM model used in the simulation of the halos of the Sgr and

MW galaxies. Our aim in this study is to analyze and describe the differences between the Sgr stream evolution using a CDM model—the only model yet considered—and self-interacting DM models.

Chapter 2

Self-interacting dark matter

2.1 Motivations

We have previously discussed the small-scale problems observed with the ΛCDM paradigm. One of the richest potential solutions comes when considering self-interacting dark matter (SIDM) models. These models introduce new mechanisms by which dark matter particles can interact with each other, beyond the gravitational interaction allowed by the CDM model.

SIDM models were first proposed in 1999 by Spergel and Steinhardt, who compiled obesrvational evidence for its existence [12]. They also performed initial simulations which found that SIDM models tend to give rise to cored halso and different small-scale structures, indicating a potential solution to the core-cusp and other small-scale problems [13]. This sparked a number of other studies of SIDM simulations which used various observational data to place constraints on the self-interaction cross section of the dark matter particles. These studies greatly constrained the cross section-to-mass ratio to a degree where the impact of self-interaction would be too small to solve the small-scale problems. As such, SIDM models fell out of favor for a while.

More recently, however, higher resolution simulations have produced revisions to the original constraints that are significantly looser, improving the viability of SIDM and re-igniting the study of these models [4]. Comparisons to observations of dwarf galaxies have shown that a self-interaction cross section-to-mass ratio of $\sigma/m \sim 0.5\text{-}1$ cm^2/g is needed. Studies of massive clusters, however, showed that something closer to $\sigma/m \sim 0.1$ cm^2/g is needed. Together, these imply that the self-interaction cross section must be velocity-dependent, such that it can admit the proper cross sections on both scales, ruling out simple SIDM

models such as a self-coupled scalar.

The only property of these self-interacting dark matter models that will come to strongly affect astrophysical observation is the cross section-to-mass ratio σ/m for two-to-two self-scattering. On astrophysical scales, the scattering rate per particle Γ scales as $\Gamma \sim (\sigma/m)\rho(r)v_{\text{rms}}$, where ρ is the local mass density and v_{rms} is the r.m.s. speed of DM particles [14]. As such, we can consider SIDM models in a general way when performing N-body simulations. This also yields a large freedom in the models which can be consistent with observation. Two of the most prominent models are discussed below.

2.2 Particle physics models

With little known about the precise nature of dark matter, there is a seemingly infinite number of possible theories to explore. We will discuss two of the most prominent kinds of theories.

2.2.1 Light mediator

The first is a rather simple theory that admits a rich potential phenomeonology. We let the dark matter particle be χ, a fermion with mass m_χ, charged under a spontaneously broken $U(1)$ symmetry [4]. Let the resulting gauge boson be ϕ with mass m_ϕ. Depending on the specific theory, ϕ may be a scalar or vector particle. The interaction term of the Lagrangian would then be a Yukawa coupling

$$\mathcal{L}_{\text{int}} = \begin{cases} g_\chi \overline{\chi}\gamma^\mu \chi \phi_\mu & \text{(vector mediator)} \\ g_\chi \overline{\chi}\chi\phi & \text{(scalar mediator,)} \end{cases} \tag{2.1}$$

where we let the coupling constant be g_χ. In the non-relativistic limit, such an interaction is described by the Yukawa potential [15, 16]

$$V(r) = \pm \frac{\alpha_\chi}{r} e^{-m_\phi r}, \tag{2.2}$$

where $\alpha_\chi \equiv g_\chi^2/4\pi$ is the dark fine structure constant, and the $\pm$ is set depending on whether the potential is attractive or repulsive.[1]

We can use the non-relativistic Yukawa potential above to obtain the Born differential cross section in the limit that $\alpha_\chi m_\chi/m_\phi \ll 1$. The final result is [4]

$$\frac{d\sigma}{d\Omega} = \frac{\alpha_\chi^2 m_\chi^2}{\left[m_\chi^2 v_{\text{rel}}^2 (1-\cos\theta)/2 + m_\phi^2\right]^2}. \tag{2.3}$$

An important implication of this result is that we must have $m_\phi > 0$. If instead $m_\phi = 0$, we would see $d\sigma/d\Omega \propto v_{\text{rel}}^{-4}$. This velocity dependence is far too strong

[1] For a scalar ϕ, the potential is always attractive and the sign is $(-)$. For a vector ϕ, the potential is attractive $(-)$ for $\chi\overline{\chi}$ scattering and repulsive $(+)$ for $\chi\chi$ and $\overline{\chi}\overline{\chi}$ scattering.

at small velocities to admit a solution consistent with observation. A small but nonzero m_ϕ, however, allows us to "soften" this velocity-dependence, admitting a more consistent model.

The differential cross section may also be analytically computed in the classical limit, $m_\chi v_{\rm rel}/m_\phi \ll 1$. However, exploring this model over a wider range of parameter space requires us to leave the regimes where the Born and classical approximations hold. Analytic results which hold generally outside these regimes do not exit, so there has been some work done to develop methods for approximately obtaining the results. One such method uses an the Hulthén potential, an approximation of the Yukawa potential. Another uses non-relativistic partial wave analysis to develop numerical methods that are accurate across more of phase space. There are other methods that can be considered as well; a more complete map of these methods can be found in [15].

One can use the approximation methods described above to explore various regions of phase space and to consider the velocity-dependence of the cross section that will results. For example, Figure 2.1 (left) shows the velocity-dependences of the cross section for an attractive potential in the limits considered previously, using choices for sample parameters. One can see that the Yukawa potential with a mediator particle can result in a very rich variety of velocity dependences, depending on our choice of particle physics parameters. As such, one can use astrophysical observations to constrain the phase space of these parameters. An example of such constraints is given in Figure 2.1 (right).

This model is admittedly rather simple, but it has been shown in [15] that it is possible for it simultaneously accomodate all important observations and to solve the small-scale problems.

2.2.2 Strong interactions

Some of the richest theories for self-interacting dark matter candidates that one can consider are non-Abelian gauge theories where the dark matter candidates arise as composite bound states. In these theories, the self-interaction manifests as a strong interaction.

The motivation for a considering such a model comes from our experience with QCD and the visible sector [18]. For a dark matter model to be a good candidate, it must be stable over the lifetime of the Universe and be neutral under standard model phenomena. Further, we desire models in which the models exhibit strong self-interactions. These are all properties exhibited by particles in the visible sector under QCD, so it makes sense to consider a similar theory to describe our dark matter candidate. However, we do not necessarily know the gauge group or particle properties of dark matter, leaving us a great freedom to vary the model significantly. Many of the resulting models thus have interesting and unique new physics, though these details are greatly model-dependent.

The primary free parameters of models of this kind are the confinement scale,

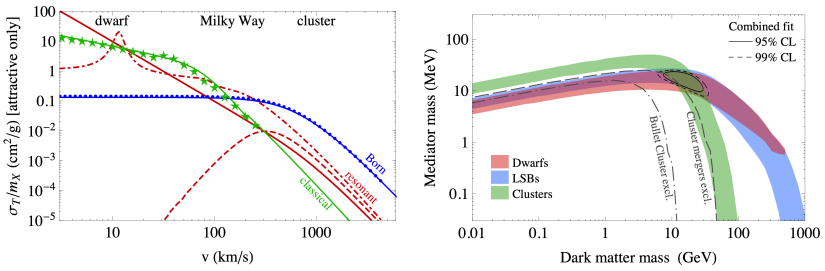

Figure 2.1: (Left) The velocity dependence of σ/m for sample parameter values (α_χ, m_χ, m_ϕ) assuming an attractive Yukawa potential. The blue, red, and green lines show the differential cross section computed under different limits; blue is the Born limit, green is classical, and red is the resonant régime, which is undiscussed in this paper. Reprinted from [16]. (Right) The parameter space for a repulsive Yukawa potential, assuming $\alpha_\chi \approx 1/137$. In colored regions are the regions of parameter space preferred by observations from dwarf galaxies (red), low surface brightness (LSB) galaxies (blue), and galaxy clusters (green). Reprinted from [17].

Λ, and the dark quark mass(es). In the event that our "dark QCD" contains no analogue to electromagentic/weak interactions, meson-like bound states of the dark quarks could be stable [19]. These mesons can be classified as loosely pion-like, where $m \ll \Lambda$, or quarkonium-like, where $m \gg \Lambda$ [18]. There are several proposed models for each of these scenarios; one of the more well-known is the strongly-interacting massive particle, or SIMP, where the dark matter candidate is pion-like and many non-Abelian theories are possible.

Our non-Abelian model may instead look quite similar to visible QCD, wherein the primary stable bound states are baryonic in nature. In [18], it is noted that the advantage of such models is that "dark matter is automatically sufficiently stable, and no further ultraviolet model-building is needed." One such dark baryon model is "Stealth Dark Matter," proposed by the LSD collaboration, which is a scalar dark baryon under a confining $SU(4)$ theory. This theory is named *stealth* dark matter because it is found that the baryons are safe from direct detection, though it does predict a spectrum of lighter meson particles that would be possible to detect at colliders [18].

The third class of candidate particles that has received attention are dark glueballs. Glueballs are bound states of only gluons, and are predicted to exist in QCD but are very difficult to detect. Dark glueballs would then be bound states of dark gluons. Such a model is possible if all the dark fermions in the theory have masses significantly larger than Λ. In this case, glueballs may become stable under an accidental symmetry like baryons, allowing them to be the primary dark matter candidate.

The observables that could result from the above considerations are as diverse

as the models themselves. One aspect of these models that we have not considered is what the interactions with the standard model could look like. Some models predict the dark matter candidate to be neutral under standard model interactions, but its constituents to be charged. In such a case, the model would have a coupling to the photon, and it would be possible to directly detect the particle. We may also consider the case where our theory predicts fundamental fermions. It is plausible that these fermions would obtain at least part of their mass through a coupling to the Higgs boson, again providing a mechanism by which we could directly detect the particles. Kribs and Neil provide more details of these observables, as well as collider-specific results, in [18].

Chapter 3

Simulations

3.1 Methodology

The following is a description of our pipeline for simulating the infall of the Sgr dSph into the Milky Way.

We generate the initial distributions of stellar and dark matter using a package called GalactICS [20]. The galaxy is modeled with a stellar disk and a dark matter halo. The halo mass density follows a Navarro-Frenk-White (NFW) distribution, [21] given by

$$\rho_{\rm halo}(r) = \frac{M_{200}}{4\pi f(c) r_{200}} \frac{cx}{r^2(1+x)^2}, \tag{3.1}$$

where M_{200} and r_{200} are the Virial mass and radius, c is the concentration parameter, r is the spherical radius, $f(c) \equiv \ln(1+c) - c/(1+c)$, and $x \equiv rc/r_{200}$.

The disk mass density follows the following distribution from [21]

$$\rho_{\rm disk}(R,z) = \left(\frac{c_0^2 M_{\rm disk}}{4\pi}\right) \frac{b_0 R^2 + (b_0 + 3\sqrt{z^2+c_0^2})(b_0+\sqrt{z^2+c_0^2})^2}{\left[R^2 + (b_0+\sqrt{z^2+c_0^2})^2\right]^{5/2} (z^2+c_0^2)^{3/2}}, \tag{3.2}$$

where R is the cylindrical radius in the plane of the disk, z is the distance from the disk's plane, $M_{\rm disk}$ is the mass of the disk, b_0 is the disk scale-radius, and c_0 is the disk scale-height.

Both of these density distributions are subject to truncation beyond a given r_t with a width of dr_t, where the truncation function is given by [22]

$$C(r; r_t, dr_t) = \frac{1}{2} \operatorname{erfc}\left(\frac{r-r_t}{\sqrt{2} dr_t}\right). \tag{3.3}$$

Parameter		MW	Sgr dSph
Halo total mass	M_{halo}	1.25×10^{12} $M_\odot$	1.3×10^{10} $M_\odot$
Halo concentration parameter	c	10	8
Halo Virial mass	M_{200}	1×10^{12} $M_\odot$	1×10^{10} $M_\odot$
Halo Virial radius	r_{200}	206 kpc	44 kpc
Halo scale-radius	r_D	??	??
Number of halo particles	N_{halo}	1.16×10^6	1.17×10^4
Disk total mass	M_{disk}	8.13×10^{10} $M_\odot$	7.8×10^{10} $M_\odot$
Disk scale-length	b_0	3.5 kpc	0.85 kpc
Disk scale-height	c_0	0.53 kpc	0.13 kpc
Number of disk particles	N_{disk}	2.03×10^6	1.95×10^4

Table 3.1: Initial conditions parameters for the Milky Way (MW) and Sagittarius (Sgr dSph) galaxies. Many of these values are taken from [11].

The disk and the halo have different values for r_t and dr_t, and each density distribution can be multiplied by the truncation function with corresponding truncation parameters to obtain the "true" density distribution.

The parameters used for the initial MW and Sgr galaxies are detailed in Table 3.1, who have compiled these results from a review of existing literature and simulations of their own. The GalactICS initial conditions are then converted to a GADGET binary initial conditions file for use in GIZMO [23, 24]—the conversion is handled by a GalactICS subpackage. SIDM runs use a public GIZMO subpackage from [14].

In order to ensure that the initial galaxies are in equilibrium, we first evolve each galaxy for 10 Gyr using GIZMO, each at rest and centered at the origin. This has uncovered some surprising trends, as the mass distribution of the galaxies has a tendency to evolve away from the initial NFW and exponential distributions. Further discussion of these trends will follow in Chapters 3.2 and 3.3.

After equilibration, the final snapshots for the Milky Way and Sagittarius galaxies are merged. The particles from the MW are centered at the origin with no initial velocity. The Sagittarius galaxy is centered at $\vec{r} = (125, 0, 0)$ kpc, with an initial velocity of $\vec{v} = (-10, 0, 70)$ km s^{-1}. The merged snapshot is then used as an initial conditions GIZMO file and evolved for another 10 Gyr. Snapshots are taken approximately every 0.1 Gyr. In most of these simulations, conditions similar to today are found after between 6 and 8 Gyrs of evolution.

3.2 CDM simulations

3.2.1 Initial galaxy equilibration

Before simulating the Sgr infall, we evolved the MW and Sgr galaxies individually for 10 Gyr such that each galaxy would be equilibrated. This is done to

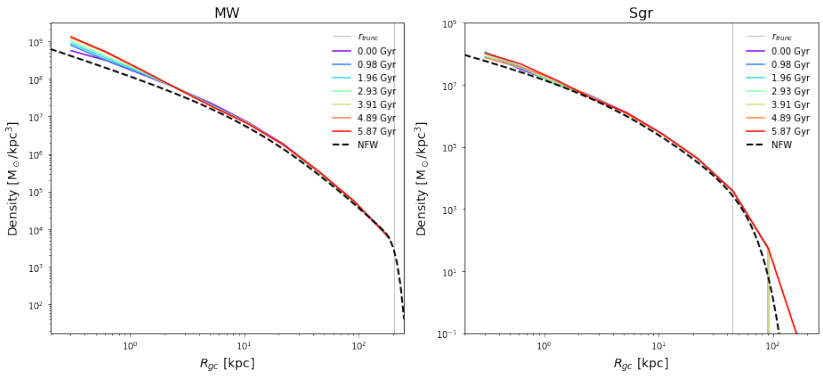

Figure 3.1: Plotted are the halo mass density distributions for the MW (left) and Sgr (right) galaxies during their initial, independent equilibration evolutions. Also plotted are the reference NFW distributions (dashed black line), following equation 3.1 *with* the truncation function (equation 3.3) included, and the truncation radius (vertical grey line).

ensure that any dynamical phenomena occuring during the Sgr infall is a result of MW-Sgr interactions and not due to local inequilibria. Given that the initial distributions of stellar and DM particles follow distributions which are supposed to be near-equilibrium, little change is expected during these preliminary simulations.

Interestingly, however, the galaxies show a tendency to redistribute halo mass away from the center of the halo during the first few Gyr of evolution. This is matched by a changing disk density distribution; as such, we believe this phenomenon to be the result of interaction between the halo and disk gravitational potentials. This phenomenon appears to be in line with similar trends found for gas disks in [20].

Plots of the evolutions of the mass distributions for the MW and Sgr halos are shown in Figure 3.1, where the reference NFW distributions from equation 3.1 are also plotted. While the effects of this phenomenon are unlikely to cause significant disruptions to our future results, it is an important deviation from the NFW distribution.

The evolution of the mass distributions for the MW and Sgr disks are shown in Figure 3.2. Here, the reference distribution, given in equation 3.2, is also plotted. We see an interesting trend in the evolution of the Sagittarius disk where mass is redistributed outward to radii significantly beyond the truncation radius. This could be an indication that we need to consider a larger value of r_t so that such large changes are not needed to obtain equilibrium.

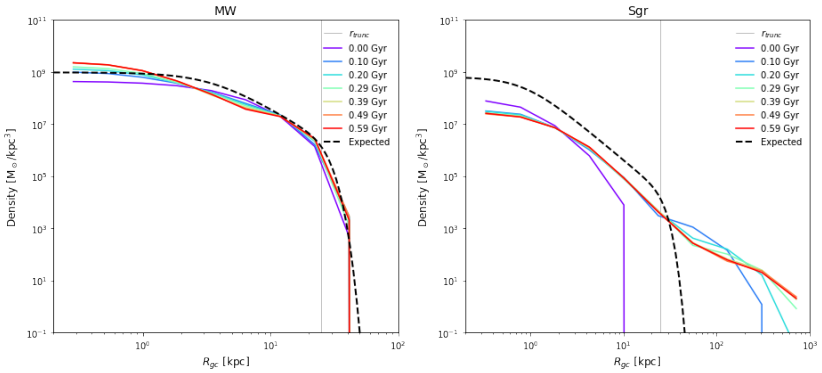

Figure 3.2: Plotted are the disk mass density distributions for the MW (left) and Sgr (right) galaxies during their initial, independent equilibration evolutions. Also plotted are the reference distributions (dashed black line), following equation 3.2 *with* the truncation function (equation 3.3) included, and the truncation radius (vertical grey line).

3.2.2 Sgr infall evolution

With the MW and Sgr galaxies equilibrated, we merge the particles of these galaxies, placing the MW at rest at the origin and the Sgr progenitor at $\vec{r} = (125, 0, 0)$ kpc with an initial velocity of $\vec{v} = (-10, 0, 70)$ km s^{-1}, following [11]. The resulting merged galaxies are then evolved for roughly 10 Gyr.

The evolution of the mass density distributions of the MW galaxy is shown in Figure 3.3. We can see that the halo distribution, while deviating away from the reference NFW distribution at low radii, remains stable throughout the evolution, implying that it had truly reached equilibrium in our previous run despite its disagreement with the reference distribution. The disk distribution also appears to remain quite stable, with the only notable changes occuring a large radii where interactions with Sgr are likely.

We can track the trajectory of the center of stellar mass of the Sgr galaxy during its infall as well. Note that this is only strongly accurate for the first few Gyr, as each tidal stripping during each orbit of the MW results in a much more disparate spread of Sgr stars after several Gyr. The trajectory is shown in Figure 3.4. Compared to [11] (e.g. their Figure 6), our model shows a significantly less smooth infall trajectory with less strongly oscillatory behavior in the separation distance.

Also following [11], we compute the observational coordinates of the simulated Sgr center-of-mass and compare to the actual observed coordinates (e.g. compare to their Figure 7). The observed coordinates are given as follows:

- $(\text{RA}, \text{dec}) = (283.83, -29.45)$ deg [25]

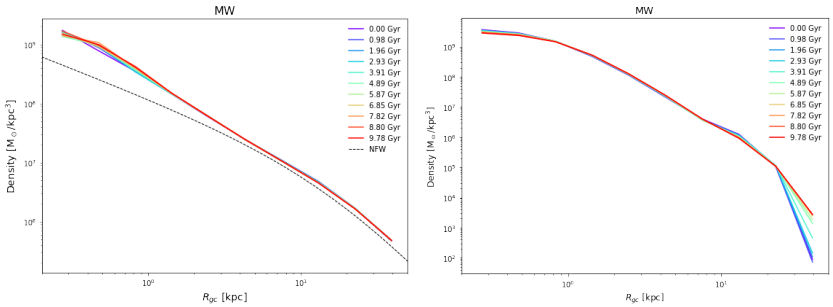

Figure 3.3: The halo (left) and disk (right) mass density distributions for the MW galaxy in the merged evolution of the MW and Sgr galaxies. The reference NFW distribution is also plotted for the halo distribution. The halo distribution remains remarkably constant, even in the low radius region where there is high deviation from the NFW distribution. The disk distribution also remains quite constant, with the only strong changes occuring at high radii, near the Sgr galaxy.

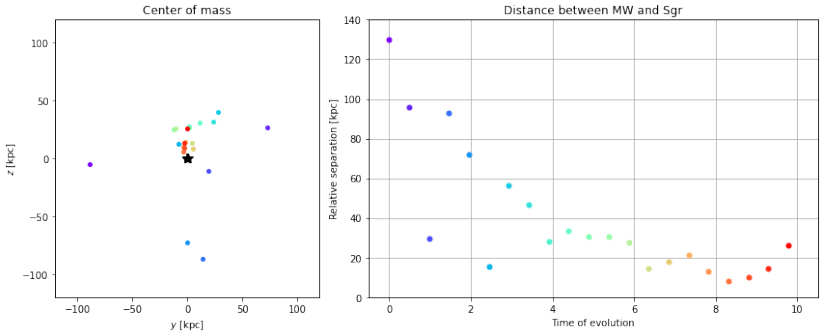

Figure 3.4: The trajectory of the Sgr center of stellar mass during its infall into the MW. Plotted on the left are the centers of stellar mass of the MW (black star) and Sgr (colored circles) over time. Plotted on the right is the separation distance between the MW and Sgr.

- Heliocentric distance $= 24.8 \pm 0.8$ kpc [7]
- $(\mu_\alpha \cos\delta, \mu_\delta) = (-2.54 \pm 0.18, -1.19 \pm 0.16)$ mas/yr [26]
- $\langle V_r \rangle$(radial velocity) $= 139.4 \pm 0.6$ km/s [27]

The results are plotted in Figure 3.5. None of our simulation snapshots attain similar coordinates to the observed coordinates, unlike [11]. Solving these discrepancies will likely require re-simulation or better time resolution in our analysis.

The above plots allow us to conclude that our simulation did not yield any

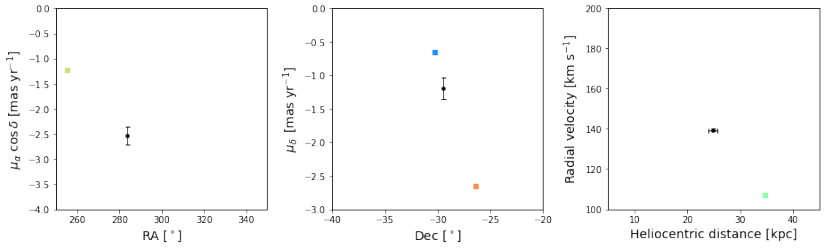

Figure 3.5: The observed coordinates of Sgr as well as the coordinates of the simulated Sgr in our snapshots. Axis limits are set such that only snapshots with reasonably-close values to the accepted observations are shown. No single snapshot falls within these ranges for more than one of the plotted coordinate pairs. Observed coordinates come from [25, 7, 26, 27].

best-fit snapshots that were remarkably similar to the position of Sgr today. As such, it is difficult to draw quantitative conclusions about the stream today. However, the resulting stream qualitatively agrees well with the results of other models, such as [11]. See Figures 3.6 and 3.7 for illustrations of the Sgr star and dark matter particles over time.

3.3 SIDM simulations

Note to reader: at this stage in my research, I have not yet completed SIDM simulations, owing primarily to a number of complications that have occurred with GIZMO. As such, in this and the following sections I will only describe the analysis that I intend to do.

3.3.1 Initial galaxy equilibration

The SIDM simulations are performed using much the same pipeline as with the CDM simulations. In particular, we create the individual MW and Sgr galaxies and evolve each independently for 5-10 Gyr to ensure equilibration before merging. The halo and disk particles are drawn from the same mass distributions as discussed previously.

For SIDM, the initial equilibration evolution is more important to track than for CDM, as the introduction of self-interaction with too high or low a cross section could strongly disturb the stability of our galaxies. We begin with a cross section of around $\sigma/m = 1$ cm^2/g, similar to that discussed in Section 2. The evolution of the halo and disk density distributions will be given in a Figure, alongside a discussion of their implications.

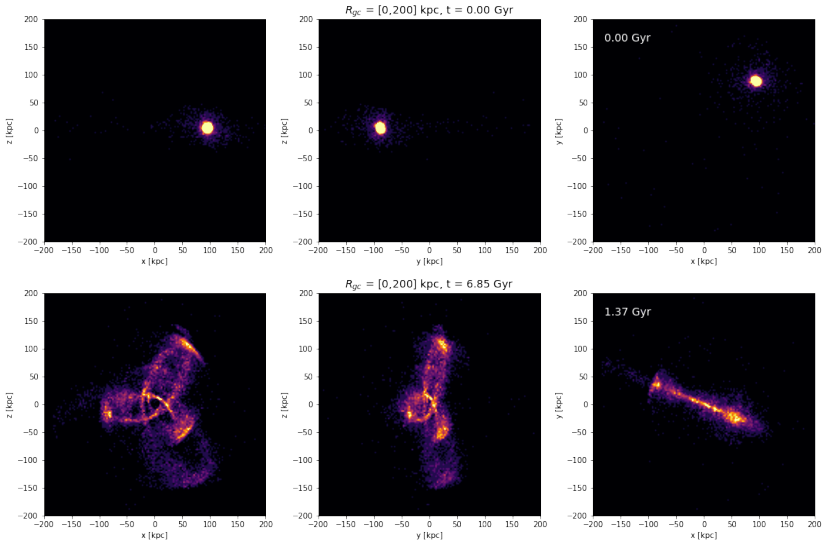

Figure 3.6: The positions of the the Sgr star particles at 0 Gyr of evolution (top) and 6.85 Gyr of evolution (bottom). These plots qualitatively agree with expected results, showing the triaxial stream distribution.

3.3.2 Sgr infall evolution

With a well-tuned cross section and equilibrated individual galaxies, we merge the galaxies as was done previously and evolve them for 10 Gyr.

Here will follow a discussion of results similar to those discussed for CDM (evolution of the MW mass distributions, trajectory of the Sgr center of mass, evaluation of observable coordinates, and illustrations of the Sgr DM/star particles). Further, I intend to measure quantitative properties of the Sgr stream (e.g. velocity dispersion, etc.) and compare to the CDM results.

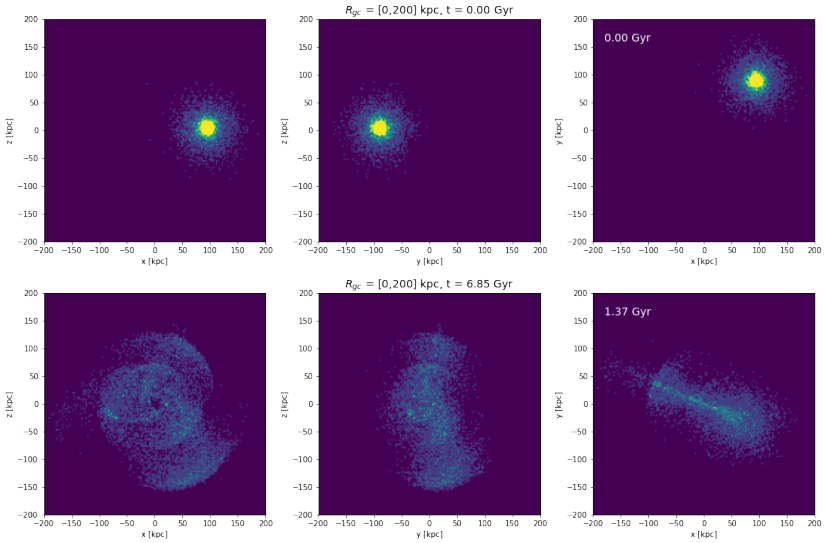

Figure 3.7: The positions of the the Sgr dark matter particles at 0 Gyr of evolution (top) and 6.85 Gyr of evolution (bottom). These plots qualitatively agree with expected results, showing the triaxial stream distribution.

Chapter 4

Comparison to Gaia data

In this section, I will compare my simulation results for both the CDM and SIDM evolved streams to data. In particular, I intend to compare the snapshots featuring the Sgr most similar to today (determined via observable coordinates) to Sgr candidates from the Gaia DR2 survey as identified by [28]. This will involve the comparison of stream properties, observable coordinates, and more, wherever possible. Without the SIDM runs completed, however, there is little more that can be discussed at this time.

Chapter 5

Conclusions

In this study, we have performed and analyzed high-resolution simulations of the infall of the Sagittarius dwarf spheroidal (Sgr dSph) galaxy into the Milky Way (MW), considering the properties of the resulting Sgr tidal stream. These analyses have been performed using both cold dark matter (CDM) and self-interacting dark matter (SIDM) models to determine where self-interaction has a strong impact on the the evolution of the stream and thereby potentially an effect on the viability of SIDM itself. We have also compared our resulting simulated Sgr streams to observed Sgr candidates from the Gaia DR2 survey.

When studies are completed, this section will be fleshed out more greatly to reflect specific discoveries made regarding the differences between the CDM and SIDM streams and their similarity to data.

Bibliography

[1] V. Trimble, "Existence and Nature of Dark Matter in the Universe," *Annu. Rev. Astron. Astrophys.*, vol. 25, pp. 425–472, Sept. 1987.

[2] W. H. Tucker, "The Mystery of the Missing Mass," in *The Star Splitters*, National Aeronautics and Space Administration, 1984.

[3] P. Schneider, J. Ehlers, and E. E. Falco, *Gravitational Lenses*. Astronomy and Astrophysics Library, Springer, 1992.

[4] S. Tulin and H.-B. Yu, "Dark Matter Self-interactions and Small Scale Structure," *Physics Reports*, vol. 730, pp. 1–57, Feb. 2018. arXiv: 1705.02358.

[5] A. W. McConnachie, "The observed properties of dwarf galaxies in and around the Local Group," *The Astronomical Journal*, vol. 144, p. 4, July 2012. arXiv: 1204.1562.

[6] R. A. Ibata, G. Gilmore, and M. J. Irwin, "A dwarf satellite galaxy in Sagittarius," *Nature*, vol. 370, pp. 194–196, July 1994.

[7] A. Kunder and B. Chaboyer, "Distance to the Sagittarius Dwarf Galaxy using MACHO Project RR Lyrae stars," *The Astronomical Journal*, vol. 137, pp. 4478–4486, May 2009. arXiv: 0903.3040.

[8] C. W. Purcell, J. S. Bullock, E. Tollerud, M. Rocha, and S. Chakrabarti, "The Sagittarius impact as an architect of spirality and outer rings in the Milky Way," *Nature*, vol. 477, pp. 301–303, Sept. 2011. arXiv: 1109.2918.

[9] D. R. Law and S. R. Majewski, "The Sagittarius Dwarf Galaxy: a Model for Evolution in a Triaxial Milky Way Halo," *ApJ*, vol. 714, pp. 229–254, May 2010. arXiv: 1003.1132.

[10] I.-G. Jiang and J. Binney, "The Orbit and Mass of the Sagittarius Dwarf Galaxy," *Monthly Notices of the Royal Astronomical Society*, vol. 314, pp. 468–474, May 2000. arXiv: astro-ph/9908025.

[11] M. Dierickx and A. Loeb, "Predicted Extension of the Sagittarius Stream to the Milky Way Virial Radius," *ApJ*, vol. 836, p. 92, Feb. 2017. arXiv: 1611.00089.

[12] D. N. Spergel and P. J. Steinhardt, "Observational evidence for self-interacting cold dark matter," *Phys. Rev. Lett.*, vol. 84, pp. 3760–3763, Apr. 2000. arXiv: astro-ph/9909386.

[13] R. Davé, D. N. Spergel, P. J. Steinhardt, and B. D. Wandelt, "Halo Properties in Cosmological Simulations of Self-Interacting Cold Dark Matter," *ApJ*, vol. 547, pp. 574–589, Feb. 2001. arXiv: astro-ph/0006218.

[14] V. H. Robles, J. S. Bullock, O. D. Elbert, A. Fitts, A. González-Samaniego, M. Boylan-Kolchin, P. F. Hopkins, C.-A. Faucher-Giguère, D. Kereš, and C. C. Hayward, "SIDM on FIRE: Hydrodynamical Self-Interacting Dark Matter simulations of low-mass dwarf galaxies," *Monthly Notices of the Royal Astronomical Society*, vol. 472, pp. 2945–2954, Dec. 2017. arXiv: 1706.07514.

[15] S. Tulin, H.-B. Yu, and K. M. Zurek, "Beyond Collisionless Dark Matter: Particle Physics Dynamics for Dark Matter Halo Structure," *Phys. Rev. D*, vol. 87, p. 115007, June 2013. arXiv: 1302.3898.

[16] S. Tulin, H.-B. Yu, and K. M. Zurek, "Resonant Dark Forces and Small Scale Structure," *Phys. Rev. Lett.*, vol. 110, p. 111301, Mar. 2013. arXiv: 1210.0900.

[17] M. Kaplinghat, S. Tulin, and H.-B. Yu, "Dark Matter Halos as Particle Colliders: A Unified Solution to Small-Scale Structure Puzzles from Dwarfs to Clusters," *Phys. Rev. Lett.*, vol. 116, p. 041302, Jan. 2016. arXiv: 1508.03339.

[18] G. D. Kribs and E. T. Neil, "Review of strongly-coupled composite dark matter models and lattice simulations," *Int. J. Mod. Phys. A*, vol. 31, p. 1643004, Aug. 2016. arXiv: 1604.04627.

[19] J. M. Cline, Z. Liu, G. D. Moore, and W. Xue, "Composite strongly interacting dark matter," *Phys. Rev. D*, vol. 90, p. 015023, July 2014. arXiv: 1312.3325.

[20] N. Deg, L. M. Widrow, T. Randriamampandry, and C. Carignan, "GalactICS with Gas," *Monthly Notices of the Royal Astronomical Society*, vol. 486, pp. 5391–5399, July 2019. arXiv: 1904.12700.

[21] H.-H. Wang, R. S. Klessen, C. P. Dullemond, F. C. v. d. Bosch, and B. Fuchs, "Equilibrium Initialization and Stability of Three-Dimensional Gas Disks," *Monthly Notices of the Royal Astronomical Society*, vol. 407, pp. 705–720, Sept. 2010. arXiv: 1004.5593.

[22] L. M. Widrow, B. Pym, and J. Dubinski, "Dynamical Blueprints for Galaxies," *ApJ*, vol. 679, pp. 1239–1259, June 2008. arXiv: 0801.3414.

[23] P. F. Hopkins, "GIZMO: A New Class of Accurate, Mesh-Free Hydrodynamic Simulation Methods," *Monthly Notices of the Royal Astronomical Society*, vol. 450, pp. 53–110, June 2015. arXiv: 1409.7395.

[24] V. Springel, "The cosmological simulation code GADGET-2," *Monthly Notices of the Royal Astronomical Society*, vol. 364, pp. 1105–1134, Dec. 2005. arXiv: astro-ph/0505010.

[25] NASA and California Institute of Technology, "NASA/IPAC Extragalactic Database: Sagittarius Dwarf Spheroidal."

[26] D. Massari, A. Bellini, F. R. Ferraro, R. P. van der Marel, J. Anderson, E. Dalessandro, and B. Lanzoni, "Hubble Space Telescope Absolute Proper Motions of NGC 6681 (M70) and the Sagittarius Dwarf Spheroidal Galaxy," *ApJ*, vol. 779, p. 81, Nov. 2013.

[27] M. Bellazzini, R. A. Ibata, S. C. Chapman, A. D. Mackey, L. Monaco, M. J. Irwin, N. F. Martin, G. F. Lewis, and E. Dalessandro, "The Nucleus of the Sagittarius dSph Galaxy and M54: A Window on the Process of Galaxy Nucleation," *The Astronomical Journal*, vol. 136, pp. 1147–1170, Sept. 2008.

[28] R. Ibata, M. Bellazzini, G. Thomas, K. Malhan, N. Martin, B. Famaey, and A. Siebert, "A panoramic landscape of the Sagittarius stream in Gaia DR2 revealed with the STREAMFINDER spyglass," *ApJ*, vol. 891, p. L19, Mar. 2020. arXiv: 2002.11121.